Acta Cryst. (1998). B**54**, 221–230

Determination of the Bonding and Valence Distribution in Inorganic Solids by the Maximum Entropy Method

G. H. Rao† and I. D. Brown*

Brockhouse Institute for Materials Research, McMaster University, Hamilton, Ontario, Canada L8S 4M1. E-mail: idbrown@mcmaster.ca

(*Received 4 August 1997; accepted 10 October 1997*)

Abstract

The distribution of valence among the bonds in the bond graph of an inorganic compound is used to calculate an 'entropy'. We show that the distribution of valence that maximizes this entropy (ME) is similar, but not identical, to that obtained using the equal-valence rule (EVR) proposed by Brown [*Acta Cryst.* (1977), B**33**, 1305–1310]. Since the ME solutions are maximally non-committal with regard to missing information, they give better predictions of the observed valence distributions than the EVR solutions when lattice constraints or electronic anisotropies are present, but worse predictions when these effects are absent. Since valences calculated using ME are necessarily positive, they give significantly better predictions in cases where EVR predicts a negative bond valence. In the absence of electronic distortions the observed bond graph is either the graph with the highest maximum entropy or it has an entropy within 1% of this value. Since the entropy depends on the oxidation states of the atoms, compounds with the same stoichiometry and cation coordination numbers but different atomic valences may adopt different bond graphs and hence different structures.

1. Introduction

Prediction of the crystal structure of a compound from the knowledge of its chemical formula and the properties of its atoms (atomic valence and coordination number) is one of the most challenging subjects in materials science and crystallography. Recently one of us has shown that the restrictions imposed by both chemistry and three-dimensional space on structures of inorganic crystals can be analysed using the bond-valence model and space-group theory (Brown, 1997) by assuming that the structure adopted has the highest possible symmetry. A full description of the bond-valence model, which has its roots in Pauling's concept of bond strength, has been given by Brown (1992*a*). In this model each atom i in an inorganic solid is assigned an atomic valence (V_i, positive or negative), which is normally equal to its oxidation state, and each atom is connected by N_i bonds to nearest neighbours that have a valence of opposite sign. Thus, the structure is represented by a network of atoms linked by bonds in which atoms with positive valence (cations) are bonded only to atoms with negative valence (anions) and *vice versa*. Bond valences, s_{ij}, can be assigned to the bonds between atoms i and atoms j under the condition that the bond-valence sum around any atom is equal to its atomic valence, *i.e.* the valence sum rule given by (1)

$$\Sigma_j s_{ij} = V_i. \qquad (1)$$

Equation (1) essentially corresponds to Pauling's electroneutrality principle. The usefulness of bond valences lies in the empirical correlation found between them and the lengths R_{ij} of the bonds as given by (2) (Brown & Shannon, 1973; Brown & Altermatt, 1985)

$$s_{ij} = \exp([R_0 - R_{ij}]/B), \qquad (2)$$

where R_0 and B are constants whose values have been determined empirically for each pair of atoms that form bonds (Brown & Altermatt, 1985; Brese & O'Keeffe, 1991).

The principle of maximum symmetry is a useful heuristic when simulating structures using the bond-valence model. It states that the observed structure is the most symmetric, consistent with the constraints acting on the system. Since the sum rule (1) is not usually sufficient to uniquely determine the distribution of valence among the bonds of the network, we can invoke the principle of maximum symmetry which implies that the valence should be distributed as uniformly as possible among the bonds. The most uniform distribution is the one in which all bonds have equal valence, but such a distribution does not in general satisfy the valence sum rule (1). One possible distribution, that which obeys (1) and minimizes the least-squares deviation from the average valence, is that

† Permanent address: Institute of Physics and Centre for Condensed Matter Physics, Chinese Academy of Sciences, Beijing 100080, People's Republic of China; e-mail: ghrao@aphy01.iphy.ac.cn.

Table 1. *Calculated and observed bond valences for $CaCrF_5$ (structure data is taken from Wu & Brown, 1973)*

	Ca−2F(1)	Ca−4F(2)	Ca−F(3)	Cr−2F(1)	Cr−2F(3)	Cr−2F(2)	σ
EVR	0.39	0.26	0.18	0.61	0.41	0.48	0.03
ME	0.36	0.26	0.22	0.64	0.39	0.47	0.04
RB	0.40	0.27	0.13	0.60	0.43	0.47	0.03
Observed	0.36 × 2	0.30 × 2	0.17	0.60 × 2	0.46 × 2	0.49 × 2	
		0.23 × 2					

Table 2. *Calculated and observed bond valences for KVO_3 (structure data is taken from Evans, 1960)*

	V−20(1)	V−20(2)	K−40(1)	K−40(1)	K−20(2)	σ
EVR	1.38	1.12	0.15	0.15	−0.12	0.14
ME	1.56	0.94	0.11	0.11	0.06	0.07
RB	1.57	0.93	0.11	0.11	0.07	0.07
Observed	1.50	0.99 × 2	0.17	0.18	0.17 × 2	
	1.47		0.12	0.06		
			0.07 × 2	0.03 × 2		

which satisfies the equal-valence rule given by (3) (Brown, 1992*b*)

$$\Sigma_{\text{loop}}\delta_{ij}s_{ij} = 0, \qquad (3)$$

where $\delta_{ij} = 1$ if the loop traverses a bond from the cation i to the anion j and $\delta_{ij} = -1$ if the bond is traversed in the opposite direction.

Equations (1) and (3), known as the network equations, are similar to the Kirchhoff laws for electrical networks and provide a unique solution for the valence distribution in the bond network. The solution thus obtained is referred to as the Equal-Valence Rule (EVR) solution. For many inorganic compounds the EVR solution agrees well with the bond valences calculated from the bond lengths in observed crystal structures (Brown, 1977, 1992*a*), as shown for example in Table 1 where the predicted and observed bond valences of $CaCrF_5$ differ by only 0.03 valence units (v.u.). However, in a number of compounds the observed bond valences differ significantly from those calculated using the network equations, as illustrated in some of the examples discussed below. There are essentially two reasons for this breakdown of the EVR: the cations may show electronic distortions (*e.g.* the Jahn–Teller effect around Cu^{2+}) or the bonds may be strained as a result of the constraints that occur when the bond graph is mapped into three-dimensional space. Electronic or lattice constraints often result in bonds having different lengths, even though they are equivalent in the connectivity table or bond graph (defined in §2). The presence of such differences in an observed structure is a strong indication of the presence of lattice constraints or electronic anisotropies. For example, in KVO_3 the six crystallographically distinct K−O(1) bonds listed in Table 2 are equivalent in the bond graph, but have observed bond valences that range from 0.03 to 0.18 v.u. The presence of lattice constraints is further indicated by the EVR prediction of a negative K−O(2) bond valence which, according to (2), is incompatible with an observed bond. Rutherford (1990) considers the calculation of a negative bond valence as a weakness of the EVR which places too much emphasis on equalizing valences around strongly bonded cations at the expense of those that are weakly bonded and he has recently explored other methods of estimating the bond valence that avoid this problem (Rutherford, 1998). In particular, he explores the Resonance-Bond model (RB) of Boisen *et al.* (1988), as well as a modification of the EVR constrained to give positive valences.

In §2 and §3 we propose an alternative approach for determining the distribution of the bond valence based on the Maximum-Entropy method (ME). Such a distribution should give a better prediction in cases where the EVR is not the only determinant of the bond lengths, as ME remains maximally non-committal to the unknown additional factors. In §4 we show that ME also provides a way of finding the most symmetric connectivity (bond graph) when there is more than one way of connecting atoms to form the bond network.

2. Bond graph and the maximum-entropy method

A crystal structure can be represented by an infinite network of atoms connected by bonds. This network can be factored into a short-range component (the arrangement of nearest neighbours) determined by the chemistry (the bonding preferences of each atom) and a long-range component determined by the translational symmetry elements of the space group (Brown, 1997). Since the bond-valence model describes only the chemistry, the long-range order need not initially be considered, although the influence of lattice constraints on the bond length may ultimately modify the geometry that would be expected from chemical considerations alone.

It is therefore sufficient when considering the initial assignment of bond valences to work with a finite connectivity graph that indicates how the atoms of a single formula unit are linked together. Such a graph, known as a *bond graph*, may be represented by diagrams such as those given in the first five figures of this paper. It is convenient to distinguish this graph, which shows how the atoms are linked, but in which all the links have equal value, from the *valence graph* which is the same graph with each bond weighted according to its valence. The purpose of the analysis described in this paper is to discover how to create the valence graph that best corresponds to the observed structure.

The maximum entropy method is widely used to reconstruct an intensity distribution of an image from a degraded or incomplete distribution. Under these circumstances the true distribution is unknown and there are many possible distributions consistent with the degraded distribution. The maximum entropy method (ME), by looking for the arrangement with the maximum configurational entropy, allows one to determine the most probable reconstructed distribution that is consistent with both the observed distribution and any other information that may be available. Such a distribution remains maximally non-committal with regard to any missing information (Daniell, 1991).

For a discrete intensity distribution of an image $\{f_i\}$, the configurational entropy of the distribution is usually defined as

$$S = -\Sigma_i f_i . \ln(f_i/m_i), \tag{4}$$

where $\{m_i\}$ is an initial estimate of the distribution representing any information about the distribution that is already known. If there is no prior knowledge of the nature of the distribution, the principle of maximum symmetry implies that a uniform distribution should be used as an initial estimate, *i.e.* all the m_i's are equal and can be set to unity.

Assuming that the bond graph is already known, which implies that we know the chemical formula and chemical connectivity, a valence graph is constructed by assigning to each bond in the bond graph a valence that is consistent with any prior knowledge of the valence distribution. The valence-sum rule (1) constitutes such prior knowledge since it is involved in the definition of the bond valence and is rarely violated in observed structures. The equal-valence rule (3), however, although obeyed in many structures, is violated when anisotropic electronic effects or lattice constraints are present and therefore cannot be presumed to hold in general. Unfortunately, the valence-sum rule does not lead directly to an initial estimate $\{m_{ij}\}$ and it must be brought in as a restriction on the values of s_{ij} when the entropy is maximized. Identifying the distribution $\{f_i\}$ with the distribution of bond valences $\{s_{ij}\}$, the configurational entropy of the valence graph is given by (5)

$$S = -\Sigma s_{ij} . \ln(s_{ij}/m_{ij}), \tag{5}$$

where the summation is over all bonds in the graph. A distribution $\{s_{ij}\}$ that obeys the valence-sum rule, but remains maximally non-committal with respect to other chemical or spatial constraints, can be derived by maximizing S subject to the valence-sum rule (1). Using the same method of undetermined multipliers that was used to derive the EVR loop equation (3) (Brown, 1992*b*), it is easy to show that S is maximized when

$$\Sigma_{\text{loop}} \delta_{ij} . \ln(s_{ij}/m_{ij}) = 0, \tag{6}$$

where the summation is made around any closed loop within the bond graph and δ_{ij} has the same values as in (3). When no prior information is available to determine the initial distribution, the principle of maximum symmetry requires $\{m_{ij}\}$ to be set to 1.0, leading to the simple equation (7)†

$$\Sigma_{\text{loop}} \delta_{ij} . \ln(s_{ij}) = 0. \tag{7}$$

Equation (7) is, therefore, the loop equation that should be used when the intent is to maximize the entropy of the valence distribution. Equations (1) and (6) or (1) and (7) thus form an alternative set of network equations that give unique solutions for any bond graph. Furthermore, the logarithmic form ensures that all the bond valences s_{ij} will be positive. The bond-valence distribution $\{s_{ij}\}$ obtained from (1) and (7) is referred to as the maximum-entropy (ME) distribution. It corresponds to the most probable and most uniform distribution of all that are consistent with the bond-valence sum rule (Daniell, 1991), whereas the EVR distribution is that which minimizes the difference between the calculated values of s_{ij} and the average of all bond valences in the structure (Brown, 1992*b*). The EVR solution is the solution that has been shown to give good predictions when electronic anisotropies and lattice constraints are absent.

Both the EVR and ME approaches define loop equations (3) and (7), respectively. The difference in the distributions calculated using these two equations can best be understood by considering the relations between the bond valences in a four-membered ring. If the valences, taken in order around the ring, are labelled as s_1, s_2, s_3 and s_4, the EVR requires that $s_1 - s_2 = s_4 - s_3$, while ME requires that $s_1/s_2 = s_4/s_3$. If

† This derivation assumes a uniform probability of all graphs in valence space, but this does not correspond to a uniform distribution in distance space because of the non-linear character of (2). Even though observations used to verify the hypotheses are necessarily made in distance space, it is the valence space that better describes the chemistry as there is no simple equivalent of the valence-sum rule in distance space. However, if it were desired to take lattice constraints into account, this would have to be done in distance space.

Table 3. *Calculated and observed bond valences for columbite AB_2O_6 (A = Mn, Fe, Co, Ni, Zn; B = Nb)*

	A—4O(1)	A—2O(2)	B—O(1)	B—2O(2)	B—3O(3)	σ(EVR)	σ(ME)	Reference
EVR	0.42	0.17	1.17	0.92	0.67			
ME	0.37	0.26	1.26	0.87	0.67			
Observed								
Mn	0.34 × 2	0.47 × 2	1.38	1.06	0.89	0.22	0.18	(*a*)
	0.26 × 2			0.60	0.60			
					0.37			
Fe	0.34 × 2	0.38 × 2	1.35	0.97	0.88	0.18	0.14	(*b*)
	0.33 × 2			0.63	0.65			
					0.37			
Co	0.31 × 2	0.39 × 2	1.16	1.10	0.94	0.19	0.17	(*a*)
	0.29 × 2			0.63	0.66			
					0.37			
Ni	0.35 × 2	0.34 × 2	1.30	1.00	0.87	0.16	0.14	(*a*)
	0.32 × 2			0.61	0.64			
					0.40			
Zn	0.37 × 2	0.40 × 2	1.25	1.04	0.93	0.19	0.16	(*c*)
	0.28 × 2			0.58	0.61			
					0.37			

(*a*) Weitzel (1976); (*b*) Bordet *et al.* (1986); (*c*) Waburg & Müller-Buschbaum (1984).

s_1 and s_2 are both large, and s_3 and s_4 are both small, the EVR will exaggerate the valence difference between the weak bonds, as pointed out by Rutherford (1990), leading in extreme cases, such as KVO_3, to the prediction of negative valences. ME, which requires only that the ratios be the same, may err in the opposite direction (*cf.* the V—O bonds in KVO_3), but will at least ensure that all bond valences are positive.

For bond graphs in which $s_1 = s_2$ and $s_4 = s_3$ for all loops, both approaches will yield the same solution. However, in these graphs the valence distribution is uniquely determined by the valence sum rule, so neither (3) nor (7) is required for a solution.

3. Examples

For all examples presented here, the bond-valence parameters R_0 and B of Brown & Altermatt (1985) are used to calculate bond valences from the observed bond lengths. All the examples discussed, apart from the first, have been chosen because the EVR does not give good predictions of the valence distributions for the reasons given below.

$CaCrF_5$ (Wu & Brown, 1973) is an example of a compound, for which the EVR approach gives an excellent prediction of the valence graph, since neither lattice strains nor electronic anisotropies are present (Brown, 1992*a*). The bond graph is shown in Fig. 1, and Table 1 compares the EVR and ME predictions with the observations. For comparison, the RB valences given by Rutherford (1998) are also shown. The root-mean-square (r.m.s.) deviation of the calculated from the observed valences (σ) shows that, while all three methods give good predictions, the EVR and RB predictions are slightly better than ME.

KVO_3 (Evans, 1960) has the bond graph shown in Fig. 2 and the EVR, ME, RB and observed valences are given in Table 2. The EVR solution for this graph gives a negative valence for the K—O(2) bond, because of the requirement that the difference between the valence of K—O(1) and K—O(2) must equal the difference of the valence between V—O(1) and V—O(2). Since the atomic valence of V is large (+5), the difference between the valence of V—O(1) and V—O(2) (~0.5 v.u.) is much larger than the valence of either K—O(1) or K—O(2), resulting in one of the K—O bonds having a negative valence. Such an EVR

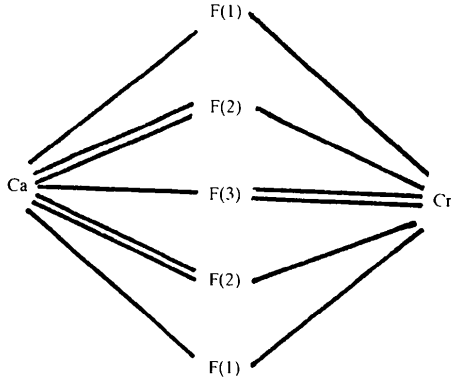

Fig. 1. Bond graph for $CaCrF_5$.

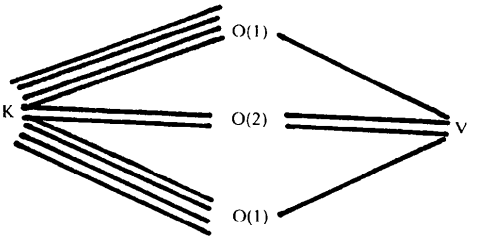

Fig. 2. Bond graph for KVO_3.

Table 4. *Calculated and observed bond valences for brannerite AB_2O_6 (A = Ca, Cd; B = V)*

The values in parentheses correspond to the bond graph neglecting the weakest V—O(2) bond (structure data are taken from Bouloux *et al.*, 1972).

	A—4O(2)	A—2O(2)	B—O(1)	B—2O(2)	B—3O(3)	σ(EVR)	σ(ME)
EVR	0.42 (0.29)	0.17 (0.43)	1.17 (1.43)	0.92 (1.57)	0.67		
ME	0.37 (0.31)	0.26 (0.37)	1.26 (1.37)	0.87 (1.63)	0.67		
Observed							
Ca	0.35 × 4	0.36 × 2	1.40	1.67 0.01	0.75 × 2 0.63	0.36 (0.07)	0.35 (0.05)
Cd	0.36 × 4	0.45 × 2	1.37	1.29 0.01	0.81 × 2 0.61	0.32 (0.12)	0.30 (0.13)

Table 5. *Calculated and observed bond valences for the Ruddlesden–Popper phase $Sr_2NdMn_2O_7$ (space group I4/mmm)*

Sr and Nd are distributed randomly over $A(1)$ in the 2(b) site and $A(2)$ in the 4(e) site. Structure data are taken from Battle *et al.* (1996).

	$A(1)$—O(1)	$A(1)$—O(3)	$A(2)$—O(2)	$A(2)$—O(3)	Mn—O(1)	Mn—O(2)	Mn—O(3)	σ
EVR	0.20	0.19	0.28	0.24	0.59	0.61	0.57	0.05
ME	0.20	0.19	0.27	0.24	0.60	0.64	0.57	0.05
Observed	0.19 × 4	0.20 × 8	0.42 0.19 × 4	0.26 × 4	0.63	0.58	0.64 × 4	

solution indicates that no K—O(2) bond should appear in the ideal bond graph, but the requirements of the three-dimensional structure bring these two atoms close enough to form a bond. As expected, the EVR predictions do not agree well with the observed valences (σ = 0.14 v.u.), while the ME and RB predictions are much better (σ = 0.07 v.u.). The failure of the EVR here is attributed to a lattice constraint whose presence is indicated by the different valences observed for the eight K—O(1) bonds which are equivalent in the bond graph.

In the columbite and brannerite $A^{2+}B_2^{5+}O_6$ structures, in which B is a d^0 transition metal, the octahedral environment of B exhibits strong out-of-centre electronic distortions as a result of a second-order Jahn–Teller effect (Kunz & Brown, 1995). This results in a violation of the equal-valence rule (3) and, in the maximum entropy method, the knowledge about the electronic distortion is treated as missing information. The bond graph for these structures is shown in Fig. 3.

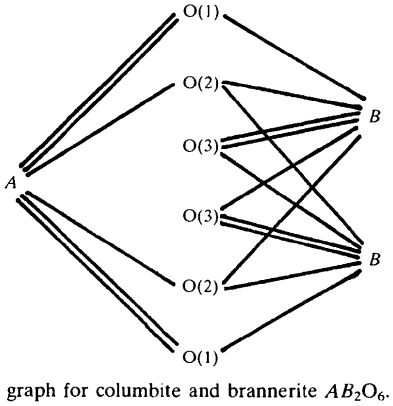

Fig. 3. Bond graph for columbite and brannerite AB_2O_6.

The bond valences shown in Tables 3 and 4 indicate that neither method gives a good prediction because of the large electronic distortion that makes the two B—O(2) bonds very different, even though they are equivalent in the bond graph and hence are predicted to have the same valence. However, the values of σ show that the ME approach gives consistently better predictions for the bond valences than the EVR approach. The variations in the bond valences observed for equivalent bonds in different columbite compounds indicate that lattice constraints are also active in this structure.

The electronic distortion in the brannerites (A = Ca, Cd; B = V; Table 4) is much larger than in the columbites. One of the two V—O(2) bonds is much weaker than the other and arguably should be excluded from the bond graph. If this is done, both the EVR and ME

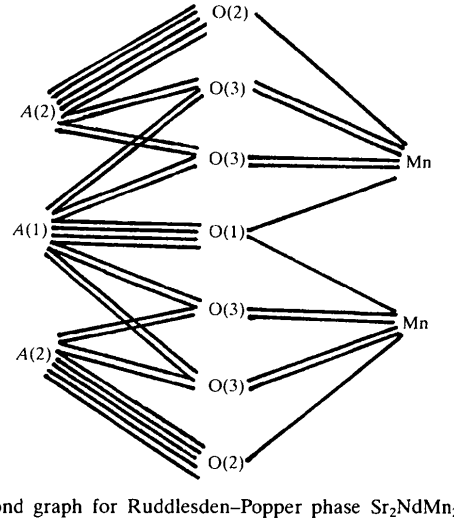

Fig. 4. Bond graph for Ruddlesden–Popper phase $Sr_2NdMn_2O_7$. Sr and Nd are randomly distributed over the $A1$ and $A2$ sites.

predictions are improved and both approaches give equally good predictions (see the values in parentheses in Table 4).

A more complex example, in which lattice constraints are expected to be present, is given in Table 5, which shows the calculated and observed valences for the bond graph (Fig. 4) of the colossal magnetoresistance Ruddlesden–Popper phase, $Sr_2NdMn_2O_7$. In spite of the lattice constraints indicated by the different valences observed for the graphically equivalent, but crystallographically distinct, $A(2)-O(2)$ bonds, both methods give a satisfactory prediction for the average of the observed valences of the $A(2)-O(2)$ bonds.

4. Choice of bond graph for structure simulation

The above analysis assumes that the bond graph is known, but in an *a priori* simulation of a crystal structure the bond graph must first be generated. The formula unit and cation coordination numbers restrict the number of possible bond graphs, but even so several graphs can usually be generated. Fig. 5 shows the complete set of bond graphs for ABX_3 compounds, in which A is eight-coordinate, B is six-coordinate, X has a coordination number between 1 and 6, and there are not more than two inequivalent X atoms. The graph expected in a real structure should be, according to the principle of maximum symmetry, the most symmetric, but what criterion should be used to rank the graphs in order of symmetry? This particular set of bond graphs is interesting because it is not easy to judge which is the most symmetric and because compounds are known that can be used to check any hypotheses.

The problem of selecting the correct graph is more complex than determining the symmetry of just the bond graph, since it is the symmetry of the valence

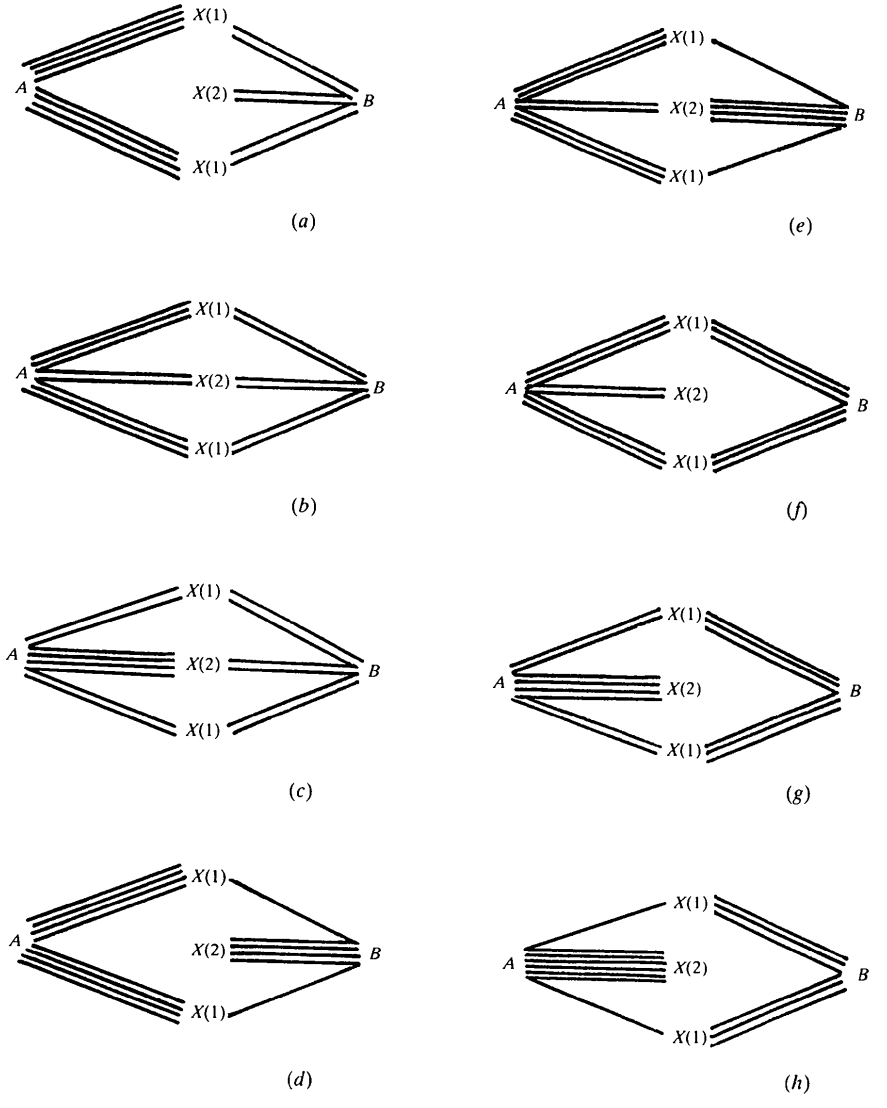

Fig. 5. Hypothetical bond graphs for ABX_3.

Table 6. *Bond-valence distribution and entropy of hypothetical bond graphs shown in Fig. 5*

Bond graph	$A-X1$	$A-X2$	$B-X1$	$B-X2$	Entropy
$B^{6+}O_3$					
a, b, c			1.0000	1.0000	0.0000†
d, e			2.0000	0.5000	−1.3863
$A^{+}B^{5+}O_3$					
a	0.1250		0.7500	1.0000	2.9425
b	0.1230	0.1310	0.8155	0.8690	2.9884†
c	0.1329	0.1172	0.8672	0.7656	2.9811
d	0.1250		1.5000	0.5000	2.2493
e	0.1511	0.0466	1.5466	0.4767	2.0629
$A^{2+}B^{4+}O_3$					
a	0.2500		0.5000	1.0000	4.1589
b	0.2417	0.2749	0.6375	0.7251	4.3835†
c	0.2808	0.2192	0.7192	0.5616	4.3537
d	0.2500		1.0000	0.5000	4.1589
e	0.2945	0.1165	1.1165	0.4417	3.8587
$A^{3+}B^{3+}O_3$					
a	0.3750		0.2500	1.0000	4.3289
b	0.3558	0.4327	0.4664	0.5673	4.9971
c	0.4430	0.3070	0.5570	0.3860	4.9316
d	0.3750		0.5000	0.5000	5.0219†
e	0.4246	0.2262	0.7262	0.3869	3.7890
f	0.1667	1.0000	0.5000		3.8712
g	0.2500	0.5000	0.5000		4.8520
h	0.5000	0.3333	0.5000		4.9698
$A^{4+}B^{2+}O_3$					
b	0.4648	0.6056	0.3028	0.3944	4.9250
c	0.6180	0.3820	0.3820	0.2361	4.8122
e	0.5333	0.4000	0.2000	0.3000	4.9224
f	0.3333	1.0000	0.3333		4.3945
g	0.5000	0.5000	0.3333		4.9698†
h	1.0000	0.3333	0.3333		4.3945
$A^{5+}B^{+}O_3$					
b	0.5686	0.7944	0.1472	0.2056	4.0706
c	0.8042	0.4458	0.1958	0.1085	3.9007
e	0.6137	0.6589	0.1589	0.1706	4.1390†
f	0.5000	1.0000	0.1667		3.8712
g	0.7500	0.5000	0.1667		4.0411
h	1.5000	0.3333	0.1667		2.7726
$A^{6+}O_3$					
b, e, f	0.6667	1.0000			1.6219†
e, g	1.0000	0.5000			1.3863
h	2.0000	0.3333			0.5754
$B^{3+}F_3$					
a, b, c			0.5000	0.5000	2.0795†
d, e			1.0000	0.5000	1.3863
$A^{+}B^{2+}F_3$					
a	0.1250		0.2500	0.5000	4.1589
b	0.1208	0.1375	0.3187	0.3625	4.2710†
c	0.1404	0.1096	0.3596	0.2808	4.2563
d	0.1250		0.5000	0.2500	4.1589
e	0.1473	0.0583	0.5583	0.2209	4.0088
$A^{2+}B^{+}F_3$					
b	0.2324	0.3028	0.1514	0.1972	4.5419
c	0.3090	0.1910	0.1910	0.1180	4.4855
e	0.2667	0.2000	0.2000	0.1500	4.5406
f	0.1667	0.5000	0.1667		4.2767
g	0.2500	0.2500	0.1667		4.5644†
h	0.5000	0.1667	0.1667		4.2767
$A^{3+}F_3$					
b, e, f	0.3333	0.5000			2.8904†
c, g	0.5000	0.5000			2.7726
h	1.0000	0.1667			1.7918

† The highest entropy.

graph that is needed. The valence graph describes the distribution of bond valence in a bond graph and its symmetry depends on the oxidation states of the atoms as well as on the connectivity. ABX_3 compounds of the type described above are known with A atom valences of 0,† +1, +2, +3 and +4, corresponding to B atom valences of +6, +5, +4, +3 and +2, respectively, when X is oxygen or sulfur. Oxides and sulfides could also in principle exist, although none is known, with A atom valences of +5 and +6, corresponding to B atom valences of +1 and 0, respectively. In addition, halides are known with A atom valences of +1 and B atom valences of +2. The determination of the most symmetric valence graph, therefore, needs to take into account not only the number of chemically distinct atoms and their coordination numbers, but also their oxidation states (atomic valences).

There is no obvious choice for the most symmetric graph in Fig. 5, particularly when one has to take into account the distribution of valence among the bonds, although graphs *b* and *c* would probably rate high on most lists. However, the configurational entropy as defined in (5) with $\{m_{ij}\} = 1$ can be used as a convenient measure of the symmetry of a valence graph. If such an entropy is a valid measure of symmetry, the principle of maximum symmetry leads to the hypothesis that the graph with the highest such entropy will be that observed in nature.

The bond valences calculated for the graphs of Fig. 5 are listed in Table 6 for various possible combinations of the atomic valences of A and B. ME bond valences are used, because we do not know how large an effect the lattice constraints will have on the bond lengths, but EVR bond valences give the same ordering. Not all of the eight bond graphs shown in Fig. 5 are possible with all combinations of atomic valence, since some graphs contain bonds with null valence, thus effectively deleting these bonds and changing the graph so that it no longer belongs to the set being examined. For various combinations of atomic valences of A and B in ABO_3, Fig. 6 shows the relative entropies of all the graphs whose entropies lie within 2% of the graph with the highest entropy.

The strongest bonds in the graph make the largest contribution to the entropy. Thus, the entropies of graphs *a*, *b* and *c*, which have the same topology around B, will converge as the valence of A approaches zero. Under these conditions graphs *a*, *b* and *c* have a higher entropy than graphs *e* and *f*, because they form equal numbers of bonds between B and each of the three X atoms. As the valence of A increases from 0 to +6 (in the oxides and sulfides) or from 0 to +3 (in the halides), the ordering of the graphs changes, but in all cases there are two or three graphs with entropies within 1% of the highest entropy, close enough that they must be considered plausible candidates for the observed structure. Graph *b* has the highest entropy for all graphs in which the valence of A is smaller than that of B, but graphs *d*, *g* and *e* come into contention when the valence of A is equal to, or larger than, that of B.

Testing the hypothesis that the observed structure should have the bond graph corresponding to the valence distribution with the highest entropy is complicated by the fact that before a bond graph can be realized in nature it has to be mapped into a crystallographic space group. The principle of maximum symmetry applied to this mapping implies that graphs that can be mapped into space groups of high symmetry are preferred to those that can only be mapped into space groups of low symmetry. Thus, the symmetry of the space group as well as the symmetry of the valence graph must be taken into account. A technique for finding the highest symmetry space group for a given graph has been described by Brown (1997). Using this method graph *c* can be mapped into the space groups *I*4/*mcm* and *P*4/*mnm* (both of which exist as distorted perovskite structures) and graph *d* can be mapped into

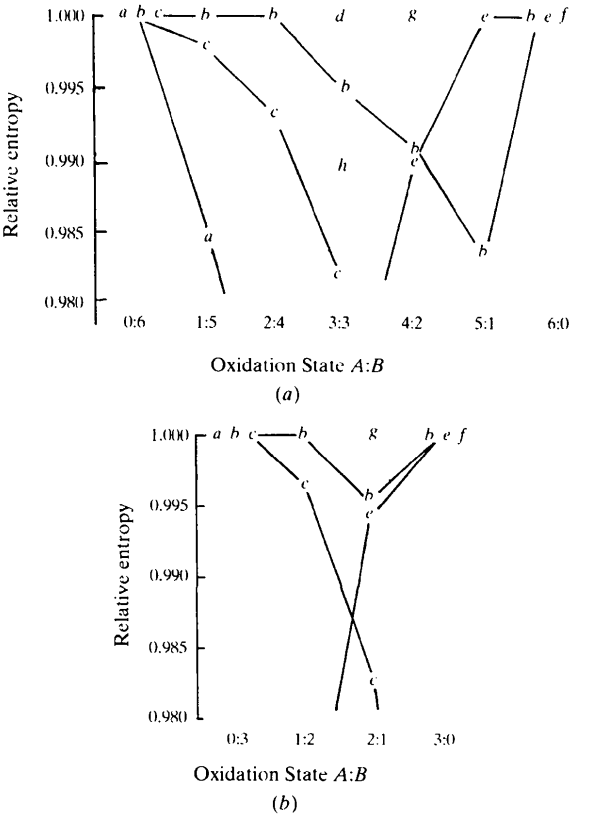

Fig. 6. The relative entropies of valence graphs shown in Fig. 5 as a function of the atomic valences of A and B in ABX_3 compounds. (*a*) X = O, S; (*b*) X = halogen.

† Valences of zero (corresponding to a missing atom) are included even though technically the resultant graph does not belong to the set of graphs being considered. However, these graphs represent natural end members of the series and the compound WO_3 is known.

the space group *P4/mmm*. Of the remainder, graphs *a* and *f* need not be considered as they have low entropies for all systems, and graph *h* is impossible to map into three-dimensional space because of the six bonds found between *A* and *X*2. An analysis of the possible site symmetries of the *A* and *B* atoms in the remaining graphs, *b*, *g* and *e*, shows that they cannot be mapped into special positions with site symmetries of order greater than 4 and so the graphs can only be found in space groups of low symmetry. From the point of view of space-group symmetry, therefore, graphs *c* and *d* are preferred to graphs *b*, *g* and *e*.

In addition to the space-group symmetry, one also needs to consider which graphs give rise to favourable packing of the atoms, since structures that bring non-bonded atoms too close, or are limited by lattice constraints, will be less favourable than those where the ideal bond distances can be realized without strain. Graphs *a*, *b* and *c* are compatible with the corner-sharing octahedra found in distorted perovskite structures, but are also compatible with the hexagonal perovskites in which some (or all) of the octahedra share faces. Graphs *d* and *e* require the octahedra to form tetragonal layers in which each octahedron shares four equatorial edges with its neighbours, leaving two terminal $B-X1$ bonds pointing along the fourfold axis. Graphs *f*, *g* and *h* can be mapped into structures in which the octahedra share six edges to form trigonal layers similar to those found in $CdCl_2$ or MoS_2. For oxides and fluorides, face- and edge-sharing octahedra bring the *B* atoms into close contact and are therefore less favourable than corner-sharing arrangements. Thus, the spatial arrangements available to the octahedra favour graphs *a*, *b* and *c* over *d*, *e*, *f* and *g*.

When all these factors are considered together, there is no compound in which the graph with the highest entropy has corner-sharing octahedra in a high-symmetry space group. Graph *b* has low crystallographic symmetry, graph *c* never has the highest entropy and graphs *d*, *e* and *g* all involve edge-sharing octahedra.

Most of the known ABX_3 compounds with eight-coordinate *A* and six-coordinate *B* have *A* atoms whose valence is less than or equal to that of *B* and most adopt a distorted perovskite structure. These have been conveniently summarized by Woodward (1997). The majority are found with graph *b* in space group *Pbnm*. However, other structures are known. Graph *c*, although never having the highest entropy, can crystallize in space groups with high symmetry. A few oxides and halides are found to crystallize in graph *c*, whose entropy lies within 1% of the entropy of the most symmetric graph (*b*) when the valence of *A* is smaller than that of *B*. Significantly, graph *c* is not found for oxides and sulfides in which *A* has a valence of +3, since its entropy is more than 1.0% smaller than that of either the highest symmetry graph *d* or the observed graph *b*. Although graph *d* can crystallize in a high-symmetry space group (*P4/mmm*), the octahedra are required to share edges, resulting in $B-B$ repulsions that can only be relieved by an unfavourable tetragonal distortion of the octahedra. Graph *d* is unknown for $A^{3+}B^{3+}X_3$ compounds, but is found for NH_4HgCl_3. For this compound, in which the valence of *A* is +1 and *B* is +2, the entropy of graph *d* is 2.6% lower than the entropy of the highest symmetry graph *b*. However, graph *d* is acceptable, because its tetragonally distorted octahedron is an environment particularly favoured by the electronic structure of Hg^{2+} and the cubic environment of NH_4^+ is particularly favourable for the formation of hydrogen bonds. Compounds in which *A* has a larger valence than *B* are rare. The only example in this series that we have found is $UFeS_3$, which adopts graph *b* in space group *Cmcm* rather than the higher entropy graph *g* that requires edge-sharing octahedra.

It should be noted that the columbite and brannerite structures also adopt a bond graph that is clearly not the most symmetric. The trirutile structure adopts a more symmetric graph (S = 4.021), but the low-symmetry graph shown in Fig. 3 (S = 3.635) is stabilized by the electronic distortions of the d^0 Nb^{5+} and V^{5+} ions (Kunz & Brown, 1995).

The above analysis shows that the entropy of a valence graph can be taken as a measure of its symmetry, but it is not the only factor that needs to be considered when modelling a structure. The ability of a graph to be mapped into a space group of high symmetry or to lead to a more favourable packing of the atoms may result in a lower entropy graph being observed, but in all the cases we have examined all the observed graphs have entropies that are within 1% of the entropy of the most symmetric graph, except where the resultant distortion is stabilized by an electronic anisotropy in one of the cations.

5. Discussion

The construction of a valence graph is an important step for structure simulation based on the bond-valence model. In such a simulation it is necessary to select the most symmetric valence graph compatible with the atomic valences and coordination numbers. The configuration entropy of the bond valence distribution provides an operational measure of the symmetry of a valence graph, leading to the expectation that the valence graph with the highest entropy is the one most likely to occur. However, if the space-group symmetry of a structure is high or the packing more favourable, graphs with entropy as much as 1% below the maximum may be found. Only when cations with electronic asymmetry are present have we found graphs with entropy less than 99% of the entropy of the most symmetric graph.

Once the bond graph has been selected, given the valence-sum rule and the principle of maximum symmetry, both the EVR and ME predict a uniform bond-valence distribution but with somewhat different biases. An EVR solution corresponds to a least-squares minimization of the deviation of the bond valences from their global as well as local averages subject to the bond-valence sum rule (Brown, 1992*b*). A ME solution is biased by a statistical probability, *i.e.* the ME solution is the most probable among all solutions compatible with known information (here, the bond-valence sum rule and the principle of maximum symmetry, but explicitly recognizing that there may be other constraints that are not known; Daniell, 1991). If it is known that electronic anisotropies or lattice constraints are absent, the EVR gives a better prediction, while ME gives a better prediction if these constraints are present but their extent is not known. Nevertheless, it is expected that the EVR and ME solutions will be close to each other for most structures, as shown in the above examples. As pointed out by Rutherford (1990), the EVR approach can place too much emphasis on equalizing valences around strongly bonded cations, resulting in negative valences for some bonds around weakly bonded cations. For such graphs ME, which ensures all bond valences are positive, produces a valence distribution closer to that observed. However, there are other methods, in particular the RB method, which are able to give predictions that agree well with observation, but avoid the problem of negative valences (Rutherford, 1998).

Neither the EVR nor ME provides a satisfactory prediction of the bond valences for the structures with strong electronic distortions, although the ME solution is slightly better, as would be expected from the assumptions underlying the two models. In these cases the graph itself may be one that matches the electronic distortions and so may be a graph with relatively low entropy. If the influence of electronic anisotropy on the bond-valence distribution can be described quantitatively, say by defining an estimated distribution $\{m_{ij}\}$, it may be possible to use ME to derive the bond-valence distribution using (6) following the procedure proposed by Kunz & Brown (1995). The new ME distribution of the bond valence would obey the valence-sum rule and be consistent with the knowledge of the electronic anisotropy, but it would still remain maximally non-committal to any as yet unknown lattice constraints.

GHR thanks the Chinese Academy of Sciences for the financial support for his 6 months sabbatical leave at McMaster University, Canada. IDB thanks the Natural Science and Engineering Research Council for a research grant.

References

Battle, P. D., Green, M. A., Laskey, N. S., Millurb, J. E., Radaclli, P. G., Rosseinsky, M. J., Sullivan, S. P. & Vente, J. F. (1996). *Phys. Rev. B*, **54**, 15967–15977.

Boisen, M. B. Jr, Gibbs, G. V. & Zhang, Z. G. (1988). *Phys. Chem. Miner.* **15**, 409–415.

Bordet, P., McHale, A., Santoro, A. & Roth, R. S. (1986). *J. Solid State Chem.* **64**, 30–46.

Bouloux, J. C., Perez, G. & Galy, J. (1972). *Bull. Soc. Fr. Mineral. Cristallogr.* **95**, 130–133.

Brese, N. E. & O'Keeffe, M. (1991). *Acta Cryst.* A**47**, 192–197.

Brown, I. D. (1977). *Acta Cryst.* B**33**, 1305–1310.

Brown, I. D. (1992*a*). *Acta Cryst.* B**44**, 553–572.

Brown, I. D. (1992*b*). *Z. Kristallogr.* **199**, 255–272.

Brown, I. D. (1997). *Acta Cryst.* B**53**, 381–393.

Brown, I. D. & Altermatt, D. (1985). *Acta Cryst.* B**41**, 244–247.

Brown, I. D. & Shannon, R. D. (1973). *Acta Cryst.* A**29**, 266–282.

Daniell, G. J. (1991). *Maximum Entropy in Action*, edited by B. Buck & V. A. Macaulay, pp. 1–18. Oxford: Clarendon Press.

Evans, H. T. Jr (1960). *Z. Kristallogr.* **114**, 257–277.

Kunz, M. & Brown, I. D. (1995). *J. Solid State Chem.* **115**, 295–406.

Rutherford, J. S. (1990). *Acta Cryst.* B**46**, 289–292.

Rutherford, J. S. (1998). *Acta Cryst.* B**54**, 204–210.

Waburg, M. & Müller-Buschbaum, H. Z. (1984). *Z. Anorg. Allg. Chem.* **508**, 55–60.

Weitzel, H. (1976). *Z. Kristallogr.* **144**, 238–258.

Woodward, P. M. (1997). *Acta Cryst.* B**53**, 44–46.

Wu, K. K. & Brown, I. D. (1973). *Mater. Res. Bull.* **8**, 593–598.